Investigation of Acidulation and Coating of Saudi Phosphate Rocks. 2. Continuous Acidulation

ARTICLE *in* INDUSTRIAL & ENGINEERING CHEMISTRY RESEARCH · NOVEMBER 1995

Impact Factor: 2.59 · DOI: 10.1021/ie00038a057

5 AUTHORS, INCLUDING:

Morteza Ghasem

Iran University of Science and Technology

26 PUBLICATIONS **89** CITATIONS

SEE PROFILE

Investigation of Acidulation and Coating of Saudi Phosphate Rocks. 2. Continuous Acidulation

Said. S. E. H. Elnashaie,* Tariq F. Al-Fariss, Farag A. Aleem, Salah M. Abdel Razik, and Nayef M. Ghasem

Phosphoric Acid Group, CPAG, Chemical Engineering Department, College of Engineering, King Saud University, P.O. Box 800, Riyadh 11421, Saudi Arabia

In this paper the investigation in part 1 for batch acidulation using the shrinking core model is extended to the case of continuous acidulation. Three processes are investigated, namely, the dihydrate, hemihydrate, and foam processes. The effective diffusivities D_e are evaluated and compared with the values obtained from the batch experiments in part 1. The comparison reveals the degree of coating occurring in the three continuous processes investigated and thus points out the suitable techniques for the improvement of the performance of these processes.

Introduction

In the first part of this work (Elnashaie et al., 1990) batch acidulation experiments were used together with a relatively simple mathematical model, with one adjustable parameter (effective diffusivity, D_e), to investigate the acidulation of phosphate ore using sulfuric acid and sulfuric/phosphoric acid mixtures. It was found from that work that at 70 °C D_e for acidulation without coating is in the range of 10^{-6} m^2 h^{-1}. For the same temperature when coating of different extents takes place the value of D_e was found to be in the range of 3.5×10^{-9}–5×10^{-12} m^2 h^{-1}. It was also found that the value of D_e increases with the increase in temperature, increase in the agitation speed, and addition of small amounts of gypsum crystals at the early stages of acidulation.

Earlier Gioia et al. (1977) reported a value of $D_e = 7.0 \times 10^{-8}$ m^2 h^{-1} when the phosphate particles are coated by hemihydrate layers, while Shakourzadeh et al. (1980) used in their model values of D_e equal to 1.8×10^{-7} m^2 h^{-1}. In both of these works the models were not verified against experimental results, and therefore the values extracted by Elnashaie et al. (1990) from a large number of experiments under a wide range of operating conditions should be more reliable than the values given by Gioia et al. (1977) and Shakourzadeh et al. (1980).

In the present paper the investigation focuses on the continuous acidulation of Saudi phosphate ore. The mathematical model used to simulate the batch experiments is extended to describe the continuous acidulation processes. Three continuous processes are investigated, namely, the dihydrate (e.g., Becker, 1988; Earl et al., 1985, 1986; Yeo et al., 1991) hemihydrate (e.g., Becker, 1983; Nakajima, 1978; Wing, 1987), and foam (e.g., Slack, 1967; TVA, 1978) processes.

Experimental Continuous Dihydrate Unit. The experimental set-up for the dihydrate process is shown in Figure 1. It consists mainly of three subsystems: the feeding, reaction, and filtration subsystems.

The feeding subsystem consists of two parts: one for the phosphate ore (belt feeder fitted with a speed control unit) and the other for sulfuric acid feed and recycle phosphoric acid to the reactor (computerized dose pumps).

The reaction subsystem consists mainly of two agitated tanks (one acts mainly as the reactor while the other is mainly used as the crystallizer). Both tanks are interconnected via the recycle slurry pump in order to ensure perfect mixing inside the reaction section (which will be considered as a continuous stirred tank reactor (CSTR) during the theoretical analysis and modeling of this and the other two processes).

In order to achieve the required reaction temperature (70–80 °C) for this process, a thermostatic oil bath is used for each tank in the reactor section.

The interconnection between the reaction and the filtration subsystems is achieved via an adjustable slurry container (for adjusting the slurry temperature and also for intimate mixing of the slurry contents).

The filtration section receives the hot slurry in order to produce the final required phosphoric acid and at the same time enables the successive washing operation of the cake to enhance the P_2O_5 recovery and to handle the recycle acid (return acid) required by the reaction subsystem.

A continuous horizontal belt filter fabricated by Decker Co. with 0.04 m^2 effective filtration area was used.

During the start-up the temperature of the reactor rises until it reaches a value of 75–80 °C. The control system on the reactor temperature is activated as soon as the temperature reaches the desired value, and the control system which is interfaced with the computer controls the temperature at the desired level by manipulating the load of the oil heating.

Recycle acid produced in the filtration section is returned to the reactor section while samples from the product acid and gypsum are analyzed for P_2O_5 content.

Experimental Continuous Hemihydrate Unit. The designed flow sheet system for the continuous hemihydrate process (as shown in Figure 2) is very similar to that used in the dihydrate route except for the fact that only one tank is used due to the short residence time necessary for this process (2–3 h) compared to the large residence time of the dihydrate route (6–8 h) and extra heating elements are added for the acids before entering the reactor subsystem. The same interconnections were also used between the reaction subsystem in order to achieve the high temperature (90–100 °C) necessary for this process.

Experimental Continuous Foam Unit. The main interest in the foam process lies in its simplicity as well as its adaptability to the Saudi phosphate ores which

* Author to whom correspondence should be addressed. F45K006@SAKSU00.BITNET. Fax: ++(9661)4633563.

0888-5885/95/2634-4122$09.00/0

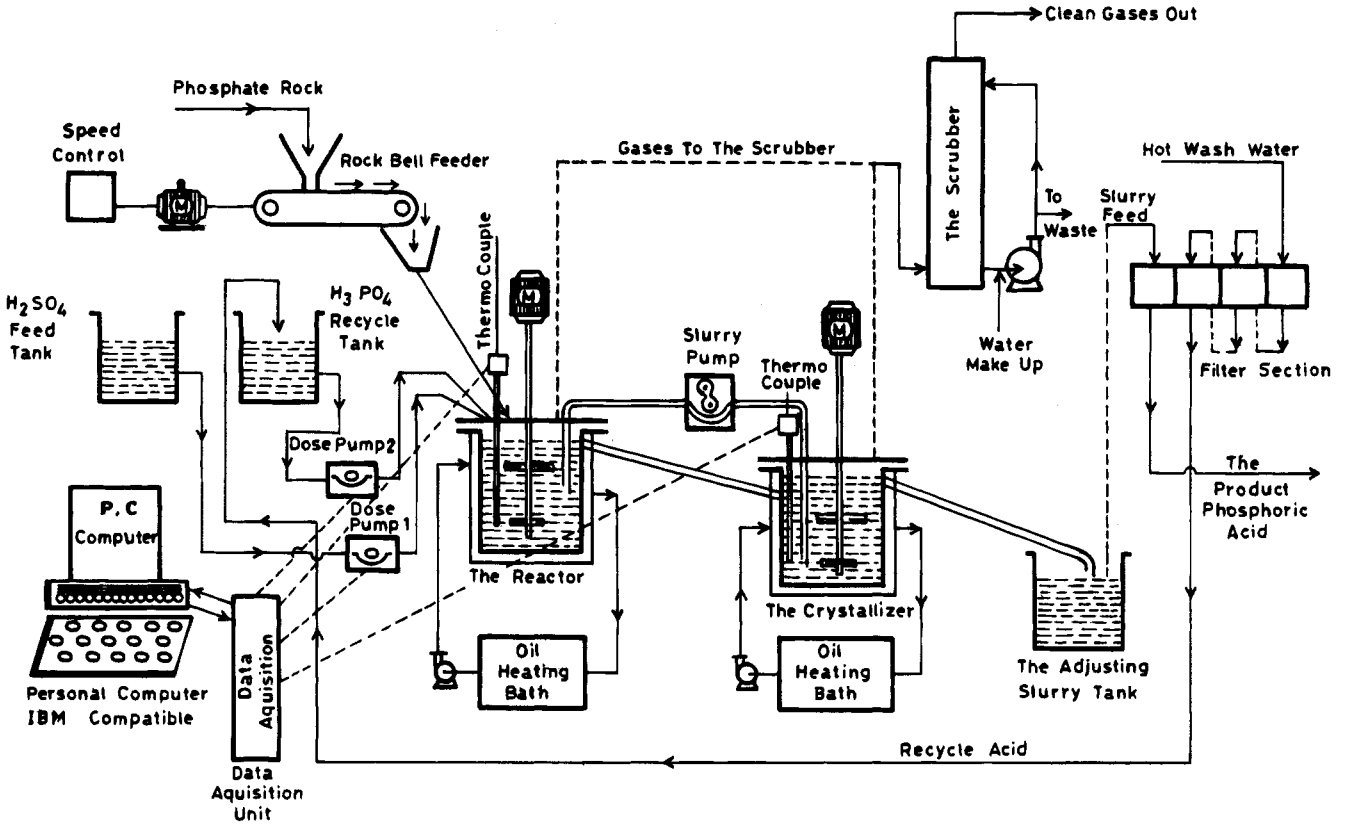

Figure 1. Experimental setup for the continuous dihydrate process.

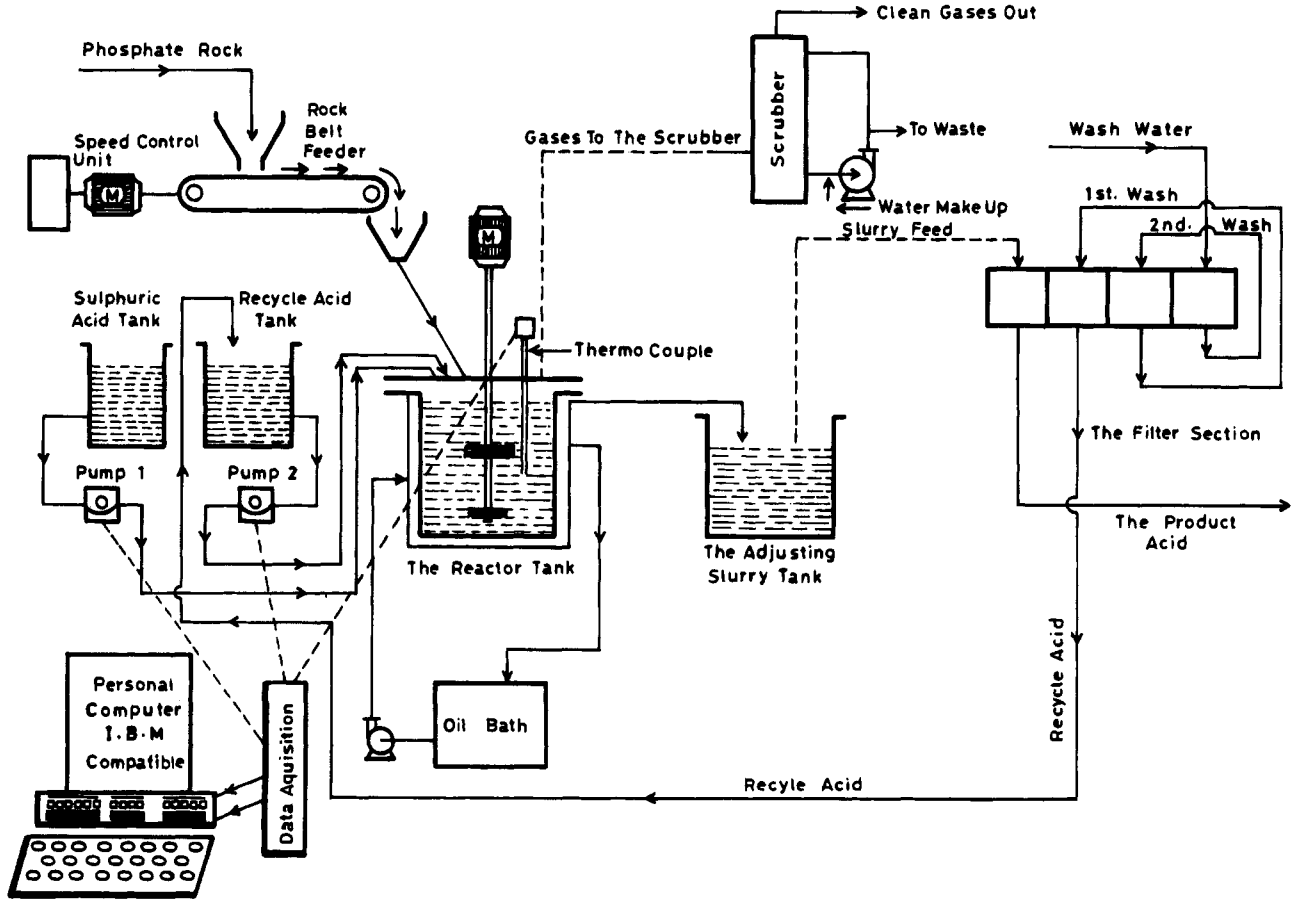

Figure 2. Experimental setup for the continuous hemihydrate process.

show high foaming tendency. In addition the process is capable of giving high concentration acid directly from the filter (up to 48–50% P_2O_5) and therefore can be used directly in the fertilizer industry without further concentration. The foam process also does not suffer from filtration problems like the hemihydrate one due to the

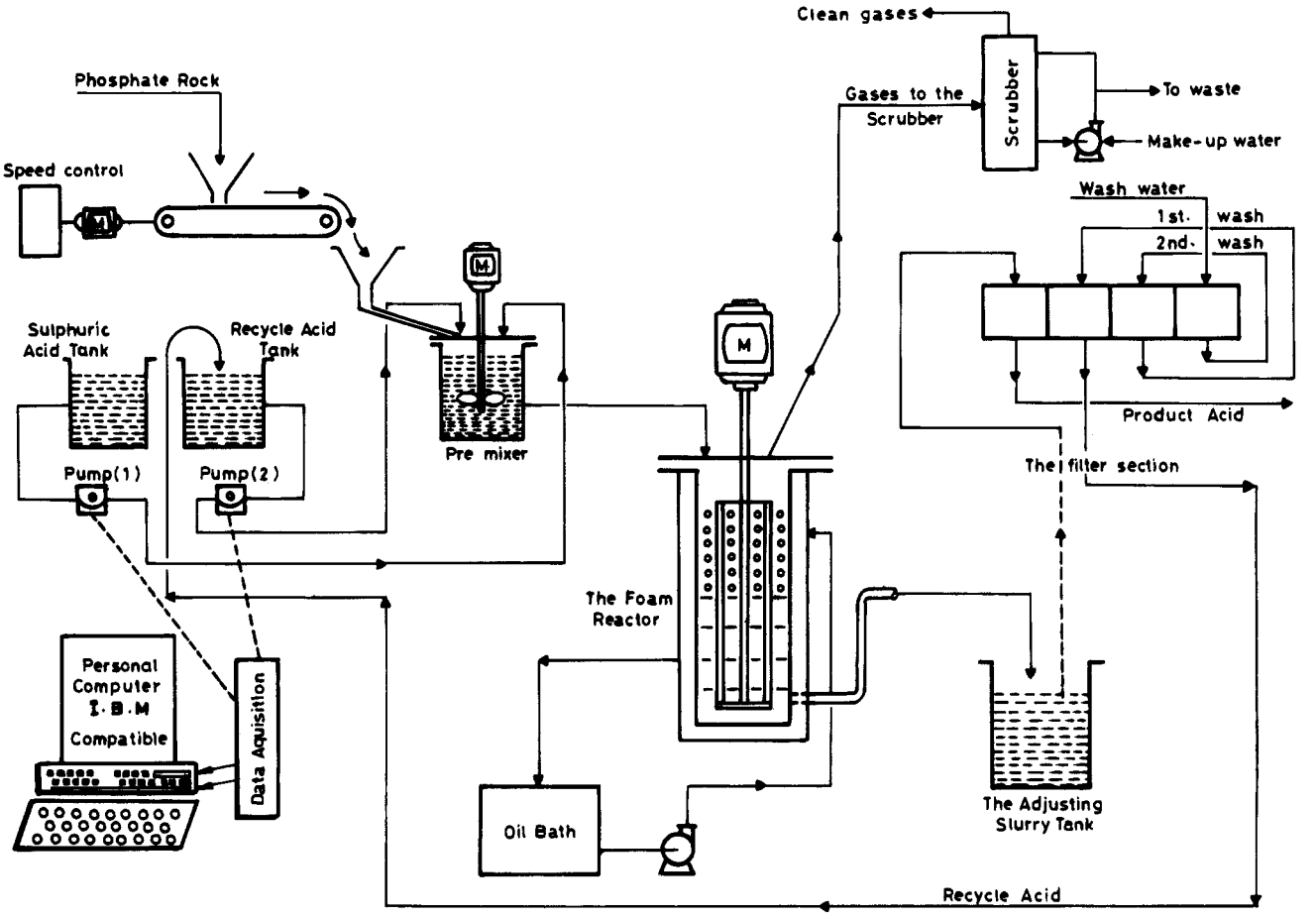

Figure 3. Experimental setup for the foam process.

role of the foam in forming agglomerates of calcium sulfate crystals which are quite easy to filter.

As shown in Figure 3, this continuous foam process is very simple. The reactor has a large length to diameter ratio in order to account for the formation of the second phase (foam layer). A hydrostatic leg is also added to the reactor exit to control the level of the interface between the foam layer and the slurry phase inside the reactor.

The Mathematical Model for the Continuous Acidulation Processes

The mathematical model developed for the batch acidulation experiments (Elnashaie et al., 1990) is extended here to the continuous acidulation case. The mass balances and physical properties relations developed for the batch acidulation are obviously all the same for the continuous acidulation. However, for the batch acidulation the change of rock conversion was described by an ordinary differential equation in time, while for the continuous acidulation the steady state rock conversion is given by an algebraic equation having the following form:

$$Y = (6.0K_{LO}C_{tx}V_R)(\phi_m\varrho_m\alpha' D_p V_L) \qquad (1)$$

where Y is the rock conversion which is related to the fluoroapatite conversion by the relation given by Elnashaie et al. (1990). Equation 1 is solved simultaneously with the mass balances and physical properties equations given earlier by Elnashaie et al. (1990) in order to obtain the steady state ore conversion Y and apatite conversion X as well as any other required state variable or physicochemical parameter.

Similar to the batch acidulation case the semiempirical diffusion coefficient D_e [used in the calculation of K_{LO} (Elnashaie et al., (1990)] is used as a single adjustable parameter in order to achieve the match between the model and the experimental results.

Results and Discussion

The Dihydrate Process. The model is matched to the three dihydrate runs which have different initial rock particle sizes, and the values of D_e which give the correct predictions are obtained. Table 1 shows that for the first run with average initial particle size of D_p = 350 μm the corresponding D_e is equal to 4.11×10^{-9} m^2 h^{-1}, while for D_p = 200 μm, $D_e = 2.76 \times 10^{-9}$ m^2 h^{-1} and for D_p = 148 μm, $D_e = 0.97 \times 10^{-9}$ m^2 h^{-1}.

These results are quite interesting because for the batch acidulation (Elnashaie et al., 1990) when the conditions were adjusted so that no coating takes place, the value obtained for the effective diffusion coefficient was $D_e = 10^{-6}$, while the D_e for the very mild coating experienced at the early stages of the batch acidulations, before severe coating had enough time to take place, was in the range 3.5×10^{-7}–3.5×10^{-9} m^2 h^{-1}. The condition of severe coating leading to almost complete blinding of the ore in the batch experiments corresponded to D_e in the range of 10^{-11}–10^{-13} m^2 h^{-1}.

This shows that the values of D_e obtained for the continuous acidulation of the three different particle sizes for the dihydrate process correspond to mild coating of the rock particles.

Table 1. Experimental and Model Results for the Continuous Dihydrate Process

variable	case number 1	2	3
ore composition, %			
P_2O_5	33.0	35.76	33.54
$Ca_5(PO_4)_3F$	76.5	76.5	76.5
$CaCO_3$	19.45	19.45	19.45
SiO_2	4.05	4.05	4.05
particle size range, μm	−425/+250	−250/+150	−250/+46
mean particle diameter (D_p), μm	350	200	148
ore feed rate, kg h^{-1}	0.83	0.83	0.83
sulfuric acid (100%) feed rate, kg h^{-1}	0.689	0.689	0.689
phosphoric acid (100%) feed rate, kg h^{-1}	0.616	0.616	0.616
water feed rate, kg h^{-1}	1.89	1.89	1.89
H_2SO_4 (100%)/ore ratio	0.865	0.865	0.865
reaction temperature, °C	78	78	78
agitation speed, rph	3×10^4	3×10^4	3×10^4
experimental conversion, %	97.0	98.5	98.0
effective diffusivity (D_e), m^2 h^{-1}	4.11×10^{-9}	2.76×10^{-9}	0.97×10^{-9}
model prediction of conversion % using D_e	97.0	98.5	98.0

Table 2. Experimental and Model Results for the Continuous Hemihydrate Process

variable	case number 1	2	3
ore composition, %			
P_2O_5	32.0	32.0	32.0
$Ca_5(PO_4)_3F$	83.0	83.0	83.0
$CaCO_3$	12.0	12.0	12.0
SiO_2	5.0	5.0	5.0
particle size range, μm	−500/+475	−500/+250	−250/+106
mean particle diameter (D_p), μm	475	375	178
ore feed rate, kg h^{-1}	1.186	1.186	1.186
sulfuric acid (100%) feed rate, kg h^{-1}	1.037	1.004	1.004
phosphoric acid (100%) feed rate, kg h^{-1}	1.147	1.147	1.147
water feed rate, kg h^{-1}	1.415	1.237	1.237
H_2SO_4 (100%)/ore ratio	0.874	0.860	0.860
reaction temperature, °C	90	90	90
agitation speed, rph	3.0×10^4	3.0×10^4	3.0×10^4
experimental conversion, %	89.0	89.3	95.87
effective diffusivity (D_e), m^2 h^{-1}	0.497×10^{-9}	0.243×10^{-9}	0.152×10^{-9}
model prediction of conversion % using D_e	89.0	89.3	95.8

The values of D_e for this process increase with the increase in ore particle size. This is due to the fact that there is competition between two tendencies in opposite directions: the fast rate of reaction due to solid fineness and the associated coating which tends to decrease D_e and therefore decrease the rate of reaction. The final effect of the dependence of the rate of acidulation on ore finesse depends upon the balance between these two factors. A much wider range of particle sizes need to be investigated in order to find the optimum particle size. The results in Table 1 suggest that $D_p = 200$ μm is the most suitable particle size among the three particle sizes used.

The Hemihydrate Process. The results of the continuous hemihydrate experiments are reported in Table 2, for three different particle sizes. For the largest particle size of 475 μm the value of D_e is 0.497×10^{-9} m^2 h^{-1}, and for the next smaller particle size of 375 μm D_e is equal to 0.243×10^{-9} m^2 h^{-1}. Further decrease of D_p to 178 μm gives $D_e = 0.152 \times 10^{-9}$ m^2 h^{-1}. Thus the same trend of increasing D_e with the increase in particle size as was observed in the dihydrate process is evident in this case. It is clear from the results that the hemihydrate process suffers from coating more severely than the dihydrate process. For the dihydrate process the average D_e for the three particle sizes is $D_{eDav} = 2.613 \times 10^{-9}$ m^2 h^{-1}, while for the hemihydrate process it is $D_{eHav} = 0.297 \times 10^{-9}$ m^2 h^{-1}; the ratio between the two values is quite high, $D_{eDav}/D_{eHav} = 8.8$.

The Foam Process. Table 3 shows the results for the foam process. For large ore particles of $D_p = 675$ μm the value of D_e is 2.12×10^{-9} m^2 h^{-1}, which is much higher than that of the hemihydrate process and comparable with D_e for the dihydrate processes. For small particle size with $D_p = 375$ μm the value of D_e decreases to 1.06×10^{-9} m^2 h^{-1} indicating, as in the other two processes, an increase in the degree of coating. For the smallest particle size ore with $D_p = 178$ μm the value of D_e decreases further to 0.448×10^{-9} m^2 h^{-1}. The average value of D_e for the foam process for the three particle sizes used is $D_{eFav} = 1.21 \times 10^{-9}$ m^2 h^{-1} which is 5 times higher than that of the hemihydrate process, but about half that of the dihydrate process. However, it is important to notice that the agitation speed for the foam process is about one-third the agitation speed of the other two processes. This points to the fact that, taking the effect of agitation speed into consideration, the foam process has intrinsically the lowest coating tendency. However, practically it is not possible to increase the agitation speed in the foam process for this will affect negatively the stability of the foam layer.

Conclusion

The preliminary results and analysis presented in this work indicate that the tendency to coating during continuous acidulation of phosphate ores is highest for the hemihydrate process followed by the dihydrate process, and that the lowest tendency to coating is associated with the foam process. The model used in this investigation, although of a high degree of empiri-

Table 3. Experimental and Model Results for the Continuous Foam Process

variable	case number 1	2	3
ore composition, %			
P_2O_5	32.0	32.0	32.0
$Ca_5(PO_4)_3F$	83.0	83.0	83.0
$CaCO_3$	12.0	12.0	12.0
SiO_2	5.0	5.0	5.0
particle size range, μm	−850/+500	−500/+250	−250/+106
mean particle diameter (D_p), μm	675	375	178
ore feed rate, kg h^{-1}	0.5	0.5	0.5
sulfuric acid (100%) feed rate, kg h^{-1}	0.460	0.460	0.460
phosphoric acid (100%) feed rate, kg h^{-1}	1.150	1.150	1.150
water feed rate, kg h^{-1}	1.05	1.05	1.05
H_2SO_4 (100%)/ore ratio	0.919	0.919	0.919
reaction temperature, °C	100.0	100.0	100.0
agitation speed, rph	1.14×10^4	1.14×10^4	1.14×10^4
experimental conversion, %	76.7	84.8	91.9
effective diffusivity (D_e), m^2 h^{-1}	2.12×10^{-9}	1.06×10^{-9}	0.448×10^{-9}
model prediction of conversion % using D_e	76.7	84.8	91.9

Table 4. Summary of the Effect of Mean Ore Particle Size on D_e for the Three Processes

dihydrate		hemihydrate		foam	
D_p, μm	$10^9 D_e$, m^2 h^{-1}	D_p, μm	$10^9 D_e$, m^2 h^{-1}	D_p, μm	$10^9 D_e$, m^2 h^{-1}
350 (−425/+250)	4.11	475 (−500/+450)	0.497	675 (−850/+500)	2.12
200 (−250/+150)	2.76	375 (−500/+250)	0.243	375 (−500/+250)	1.06
148 (−250/+46)	0.97	178 (−250/+106)	0.152	178 (−250/+106)	0.448

cism, allows the expression of these facts in a quantitative fashion. The model shows that D_{eav} for the dihydrate process is about 9 times higher than that for the hemihydrate process. For the foam process the quantification and comparison do not reveal clearly the low tendency to coating because of the low agitation speed dictated by the stability of the foam layer.

The model and the results also show that the tendency to coating increases with the decrease of ore particle size. This fact together with the fact that the intrinsic rate of reaction increases with the decrease in particle size points to the important fact that for each process and operating conditions there is an optimum particle size that gives the best performance (highest conversion). A summary of the effect of mean ore particle size on D_e for the three processes is given in Table 4 for ease of comparison. More experimental work is needed to cover a wider range of operating conditions. More mathematical modeling work is also needed in conjunction with experimental results in order to develop more elaborate less empirical phenomenological models with high predictive power without adjustable parameters.

Nomenclature

D_e = effective diffusivity,m^2 h^{-1}
D_p = mean particle diameter, μm
C_{ax} = phosphoric acid concentration at apatite conversion, X (ore conversion, Y), kg m^{-3}
C_{cx} = sulfuric acid concentration at apatite conversion, X
C_{tx} = total acid concentration ($C_{tx} = C_{ax} + C_{cx}$)
K_{LO} = mass transfer coefficient (Elnashaie et al., 1990), m h^{-1}
V_R = volume of reaction slurry, m^3
V_L= volume of the liquid phase in the reaction slurry, m^3
X = degree of fluroapatite conversion, kg kg^{-1}
Y = degree of ore conversion, kg kg^{-1}

Greek Letters

α' = part of anhydrous sulfuric acid per part of ore for stoichiometric acidulation, kg kg^{-1}
ϱ_m = density of ore, kg m^{-3}
ϕ_m = particle shape factor

Literature Cited

Becker, P. Phosphate and Phosphoric Acid. *Fertilizer Science and Technology Series*; Marcel Decker: New York, 1988; Vol. 3.

Earl, C.; Davister, A.; Thirion, F. Prayon's High Strength Double Dihydrate Phosphoric Acid Process. Davy Mckee's Answer to Cogeneration. *Phosphorus Potassium* **1985**, *140*, 31−34.

Earl, C.; Davister, A.; Thirion, F. The Davy/Prayon High Strength Phosphoric Acid Process: Cogeneration Ideal Partner. Presented at the AIChE Spring Meeting, New Orleans, April 1986; pp 1−9.

Elnashaie, S. S. E. H.; Al-Fariss, T. F.; Abdel-Razik, S. M.; Ibrahim, H. A. Investigation of Acidulation and Coating of Saudi Phosphate Rocks. 1. Batch Acidulation. *Ind. Eng. Chem. Res.* **1990**, *29*, 2389−2401.

Gioia, F; Mura, G.; Viola, A. Analysis, Simulation and Optimization of Hemihydrate Process for the Production of Phosphoric Acid from Calcareous Phosphorite. *Ind. Eng. Chem. Process Des. Dev.* **1977**, *16*, 390−399.

Nakajima, S. New Nissan High-Concentration Phosphoric Acid Process. *Chem. Econ. Eng. Rev.* **1978**, *10*, 41−45.

Shakrouzadeh, K.; Bloise, R.; Baratin, F. Modeling of a Wet-Process Phosphoric Acid Reactor. Influence of Phosphate Rock Impurities. *Proceedings International Congress on Phosphorus Compounds*; Wiley: New York, 1980; Vol. II, pp 443−454.

Slack, A. V. Phosphoric Acid. *Fertilizer Science and Technology Series*; Marcel Dekker: New York, 1967; Vol. 1.

TVA Displays Energy-Saving Phosphoric Acid Process. *Chem. Eng. News* **1978**, *13*, 32−39.

Wing, J. H. Hemihydrate Phosphoric Acid Plant Conversion at Bellendune-Canada. Presented at AIChE Meeting of Central Florida, Lakeland, FL, October 1987; pp 1−22.

Yeo, Y. K.; Cho, Y. S.; Park, W. H.; Moon, B. K. Simulation of the Dihydrate Process for the Production of Phosphoric Acid. *Korean J. Chem. Eng.* **1991**, *8*, 23−32.

Received for review November 2, 1994
Revised manuscript received May 23, 1995
Accepted June 9, 1995[⊗]

IE9406411

[⊗] Abstract published in *Advance ACS Abstracts,* July 15, 1995.